#76055
✓

①

BRIEF TESTS OF PASSIVELY VENTED BOREHOLES AT TA-54, MDA H, MDA J, AND AT TA-50, MDA C DURING 1995 AND 1996

OCTOBER, 1997

Donald A. Neeper
Science and Engineering Associates, Inc.
3205 Richards Lane, Suite A
Santa Fe, New Mexico 87505

(505) 424-6955
(505) 424-6956 fax

SEA-SF-TR-97-171

Science &
Engineering
Associates, Inc.

8985

RECEIVED
SEP 16 2003
By

BRIEF TESTS OF PASSIVELY VENTED BOREHOLES AT TA-54, MDA H, MDA J, AND AT TA-50, MDA C DURING 1995 AND 1996

D. A. Neeper

October, 1997

SUMMARY

The flow of air was monitored at nine different open boreholes in the Bandelier tuff for intervals of several days each. Seven of the boreholes responded to barometric cycles with similar flow per unit length of borehole. Two of the boreholes responded with flows 5- to 10-times larger than that of the seven. These results suggest that most boreholes in similar geologic units of the tuff will respond with predictable behavior, but that a borehole may strike a large open fracture or cavity and consequently display an unusually large flow.

CONTENTS

I. BACKGROUND

During 1995, a series of boreholes was drilled to conduct RFI phase 1 subsurface sampling at Material Disposal Areas H and J of TA-54 and C of TA-50. As part of the RFI, Field Unit 5 of the Environmental Restoration Program was also studying both passive and active vapor extraction at MDA L. (In active vapor extraction, a flow of air is forced through the ground with mechanical blowers; passive extraction utilizes natural barometric fluctuations to induce subsurface air flow.) The four disposal areas (H, J, C, and L) are located in similar strata of Bandelier tuff on Mesita del Buey. The RFI boreholes at MDAs H, J, and C were available for a few months prior to backfilling. Using available equipment, program participants sequentially monitored the passive flow at nine of the boreholes, leaving the monitoring unit at each borehole for periods of a few days to a few weeks, as other duties allowed. This passive monitoring project was designed to gain information at little added cost to the program.

The objective of this project was to learn whether passive flow would vary greatly from one hole to another as might be caused, for example, by the chance intersection of fractures by each hole.

II. DESCRIPTION OF THE BOREHOLES

The boreholes were all 4 in. diameter. Details of the drilling and geology will be presented in the RFI reports for MDAs H, J, and C. Table 1 presents the total length, angle from vertical, and Julian dates of monitoring for each borehole. Maps in Appendix A indicate the location of the boreholes.

TABLE 1. Monitored Boreholes

MDA	Borehole	Length (ft)	Angle (deg)	Monitoring dates† (Julian)	
H	54-1026	90	0	292-310	1995
J	54-1022	72	0	88- 93	1996
J	54-1019	80	30	93-100	1996
C	50-9101	117	45	319-333	1995
C	50-9100	316	0	333-347	1995
C	50-9102	110	45	347- 18	1995-96
C	54-9103	120	45	18- 32	1996
C	50-9105	120	45	32- 51	1996
C	50-9107	118	45	51- 57	1996

---

†Dates may include intervals of invalid data.

Shortly after completion of drilling and sampling, a check valve was attached to the outlet of each borehole with the intent that intervals of low atmospheric pressure would preferentially vent any remaining drill air from the formation, and pull representative pore gas into the borehole. An initial use of the flow apparatus was to test how well these valves worked. These valves were removed before conducting the flow monitoring reported here. Nonetheless, the set of nine monitored boreholes received the dubious name "burp wells," a humorous appellation that persists throughout the records of the monitoring project.

III. MONITORING APPARATUS AND PROCEDURE

The flow measuring device is illustrated schematically in Fig. 1. It consisted of a 10-ft length of PVC pipe, 2 in. diameter, mounted horizontally and connected to the surface casing of the well by an elbow. A wind screen shielded the open pipe from direct impact of the wind. The stem of an omnidirectional thermal air velocity transducer (TSI Model 8470) was mounted radially at the middle of the pipe, so that the sensing tip was located at the centerline of the pipe. In calculating volume flow rate, it was assumed that the area-average velocity was half the velocity measured at the center of the pipe when the Reynolds number was less than 1700 (laminar flow) and three-quarters the measured velocity when the Reynolds number was greater than 2400, with an interpolated average velocity at intermediate Reynolds numbers. This approximation was adequate for the comparison presented here.

Because the velocity transducer does not reveal whether flow is into or out of the borehole, two embellishments were added to the apparatus. A second velocity transducer was mounted on the pipe centerline, at the open end of the pipe. It was expected that the second transducer would experience the jet emerging from the pipe, and indicate approximately the same speed as the internal transducer during outflow. During inflow, the end transducer was expected to indicate a lower speed than the internal transducer. Although this scheme worked to some degree, it was enhanced by placing a small wedge-shaped shield just outside the sensing tip of end transducer. The shield deflected inflowing air from the tip, but minimally disturbed the outflowing air at the tip.

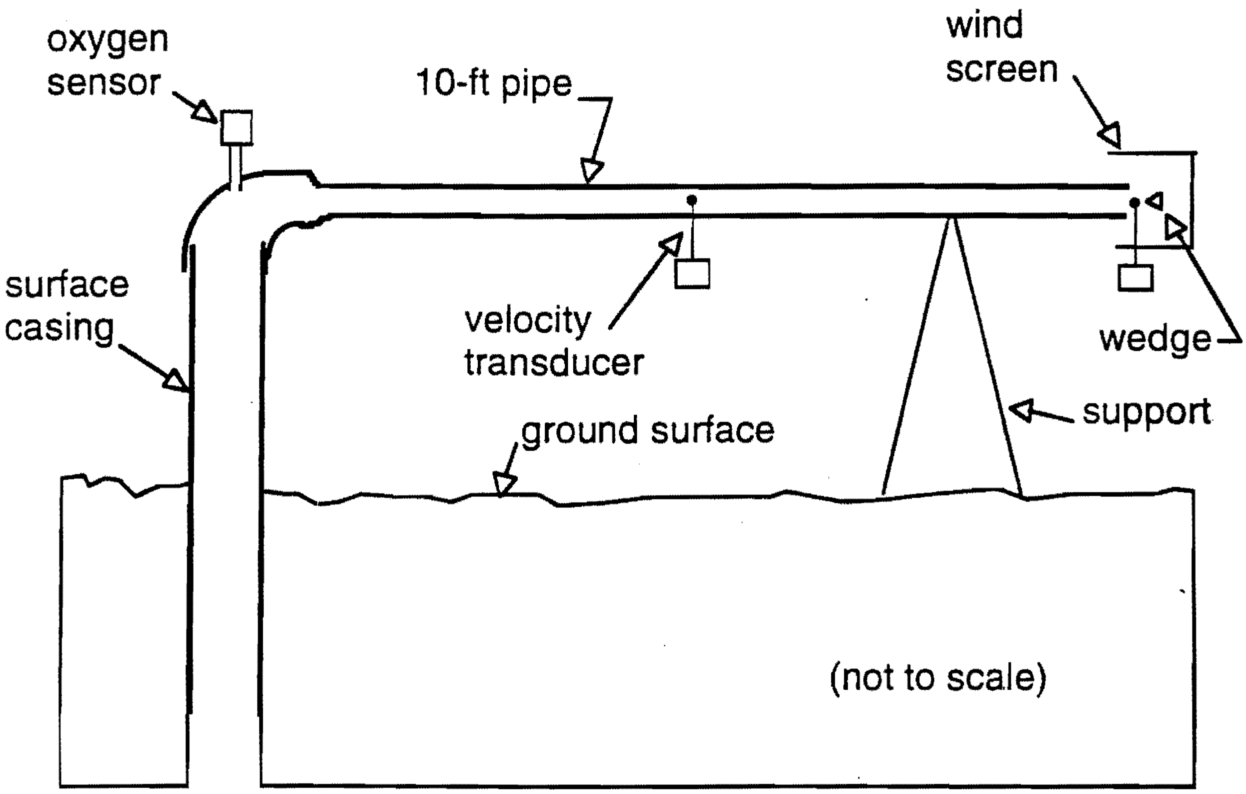

Fig. 1. FLOW MEASURING APPARATUS.

As an additional indicator of flow direction, a Figaro KE-25 oxygen sensor was connected to the pipe near the elbow. It indicated higher oxygen content during inflow than outflow. Due to the brevity of the tests and lack of time for analysis, the data from the end transducer and oxygen sensor have not been utilized to discern inflow from outflow. Rather, the data from the internal transducer were analyzed so as to compare the responses of different boreholes regardless of flow direction. However, plots of the data indicate that the end transducer and oxygen sensor worked well enough to indicate flow direction during all but the slowest flows.

Signals from the transducers were averaged during 15-minute intervals. The average air speeds and instantaneous values of atmospheric pressure, various temperatures, and instrument conditions were recorded by a Campbell 21x data logger at 15-minute intervals. Photovoltaic panels supplied electrical power.

IV. TEST RESULTS

A. Variation of Volume Flow Rate.

The objective of this project was to answer the question, "To what extent do all boreholes behave similarly in responding to barometric changes?" Various figures of merit were tried, including comparing the rate of change of barometric pressure with flow rate during large, synoptic changes. However, the instantaneous flow at any particular time is dependent both on the current change of barometric pressure and on pressure history for the previous several days. The following analytic scheme proved useful: From the available data, the analyst would select a window of a few days during which the barometric pressure was without large synoptic change. Each window was chosen so that the first and last pressures of the window were nearly equal--that is, so that the atmosphere did not induce a net flow in one direction during the window. One figure of merit was the ratio of the root-mean-square (rms) of the volume flow rate (*not* mass flow rate) to the rms variation of atmospheric pressure, normalized to borehole length. A similar figure of merit used the absolute value of the flow rate and the absolute value of the variation of barometric pressure from the average pressure. In algebraic terms, the figures of merit were:

$$F_{rms} = \frac{\sqrt{\sum v_i^2}}{\sqrt{\sum (P_i - \overline{P})^2}} \bullet \frac{1}{L}$$

$$F_{abs} = \frac{\sum |v_i|}{\sum |P_i - \overline{P}|} \bullet \frac{1}{L} ,$$

in which

F_{rms} and F_{abs} are the figures of merit for rms and absolute values of variation, respectively;

v_i is the volume flow rate during time interval i;

P_i is the atmospheric pressure during time interval i;

$\overline{P}$ is the average atmospheric pressure during the data window;

and

L is the uncased length of borehole.

F_{rms} and F_{abs} were calculated from the data for two different few-day data windows for each borehole, except for Borehole 54-1022, for which only one window of data was available due to the short period of monitoring. The bar graph of Fig. 2 compares F_{rms} and F_{abs} for the several boreholes, with a separate bar for each analytical method and each of two data windows. For example, F_{rms} 1 indicates the rms calculation at the first of two windows.

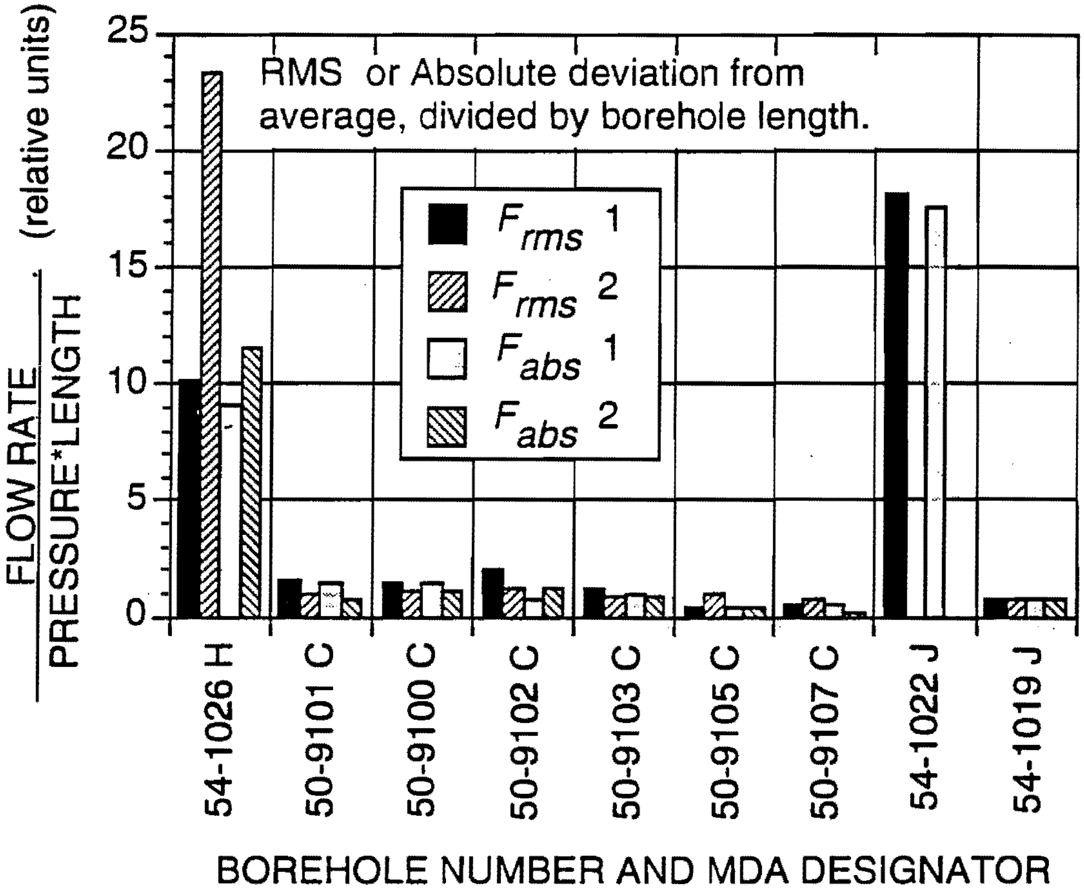

Fig. 2. FLOW RESPONSE TO BAROMETRIC VARIATION

In Fig. 2, it is apparent that seven of the boreholes behaved in approximately the same fashion, with F_{rms} and F_{abs} in the range 0.5-2.0 (relative units). In contrast, Borehole 54-1026 and 54-1022 produced flow rates roughly an order of magnitude larger than the other boreholes. Workers noted that Borehole 54-1026 consumed an inordinately large amount of cement when setting the surface casing. It is probable that the two large-flow boreholes intersected large, open fractures. A reasonable, but speculative, interpretation of Fig. 2 is that most boreholes in the lightly welded subunits of the Tshirege will display similar barometric ventilation, but occasionally a borehole may intersect an unusual fracture or cavity, and display much larger flows.

B. Instantaneous Flow Rate and Oxygen Concentration

At the seven boreholes with smaller flows, the instantaneous flow rates peaked generally in the range 0.2-2 cfm. At Borehole 54-1022, the peak instantaneous flows were in the range 1-7 cfm, and at Borehole 54-1026 the peak rates were in the range 5-15 cfm. Integrated values of the total volume exchanged on a daily basis were not calculated because meaningful values would probably require longer periods of monitoring throughout a variety of barometric conditions. The oxygen concentration in effluent gas was generally in the range 85%-100% of normal atmospheric concentration.

V. PROJECT PARTICIPANTS

Bob Gilkeson recognized the opportunity offered by the available boreholes, and directed that the project be done. D. Neeper designed the apparatus, which was constructed and fielded by Steve Limback. Tim Renn performed much of the data reduction and testing of figures of merit.

APPENDIX A

BOREHOLE LOCATIONS

Figs. A-1, A-2, and A-3 are maps showing the locations of the RFI boreholes, including the monitored boreholes, at MDA H, MDA J, and MDA C, respectively. The map of MDA C is taken from "RFI Report for Potential Release Site 50-009, MDA C," (in draft). The other maps are redrawn from informal sources, and should not be regarded as quantitatively accurate.

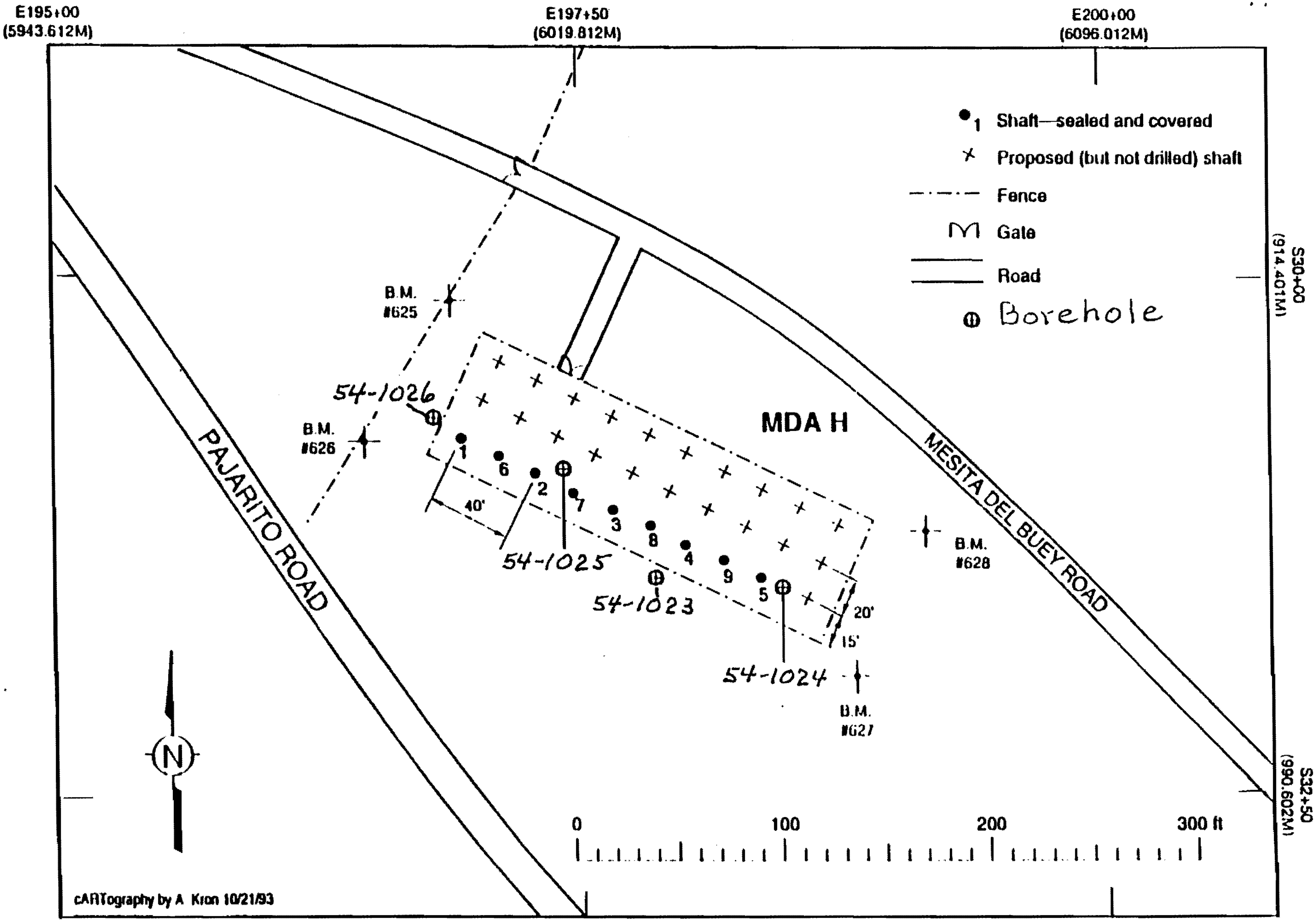

Figure A-1. Map of RFI Sampling Boreholes at MDA H.

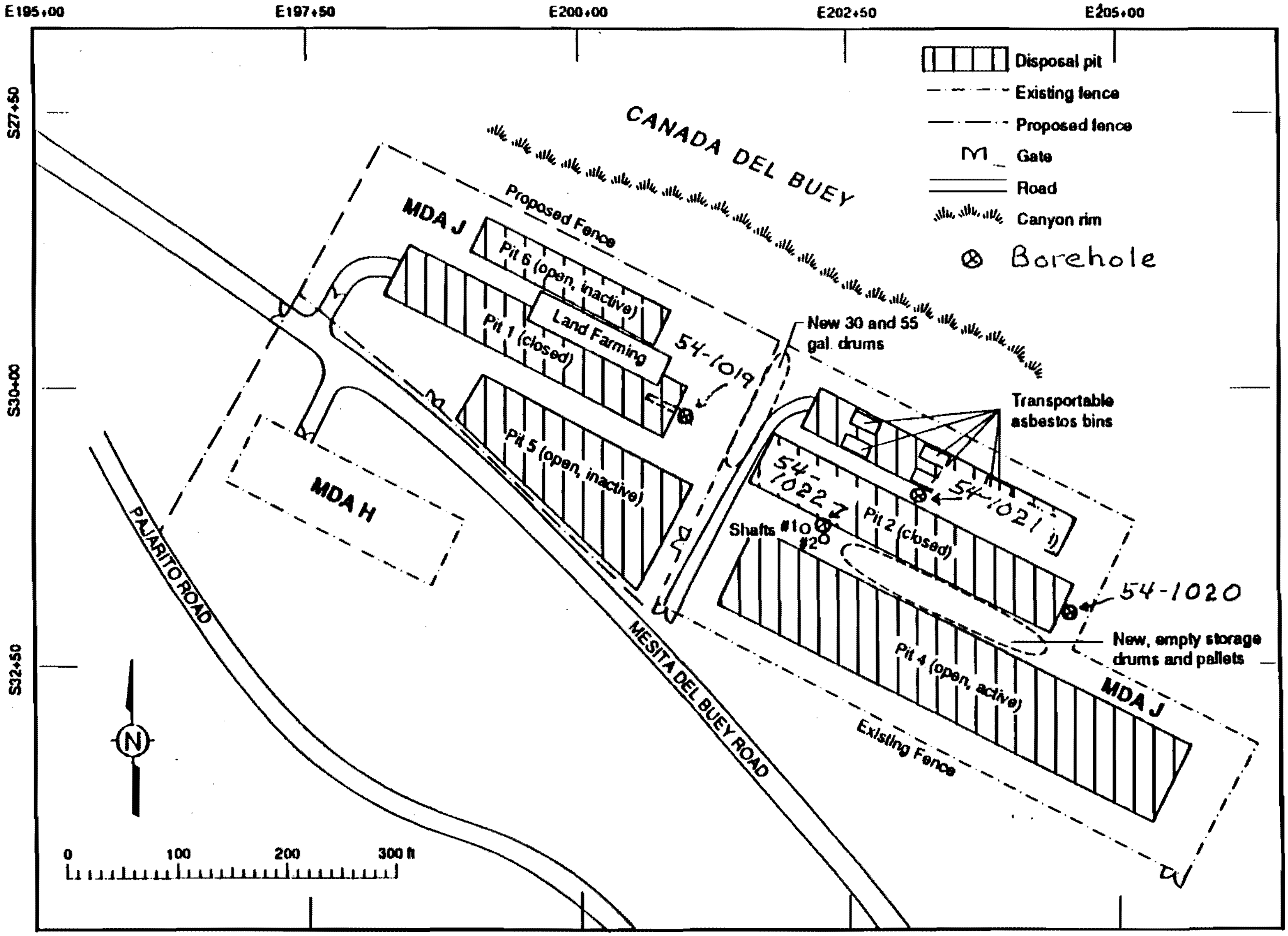

Figure A-2. Map of RFI Sampling Boreholes at MDA J.

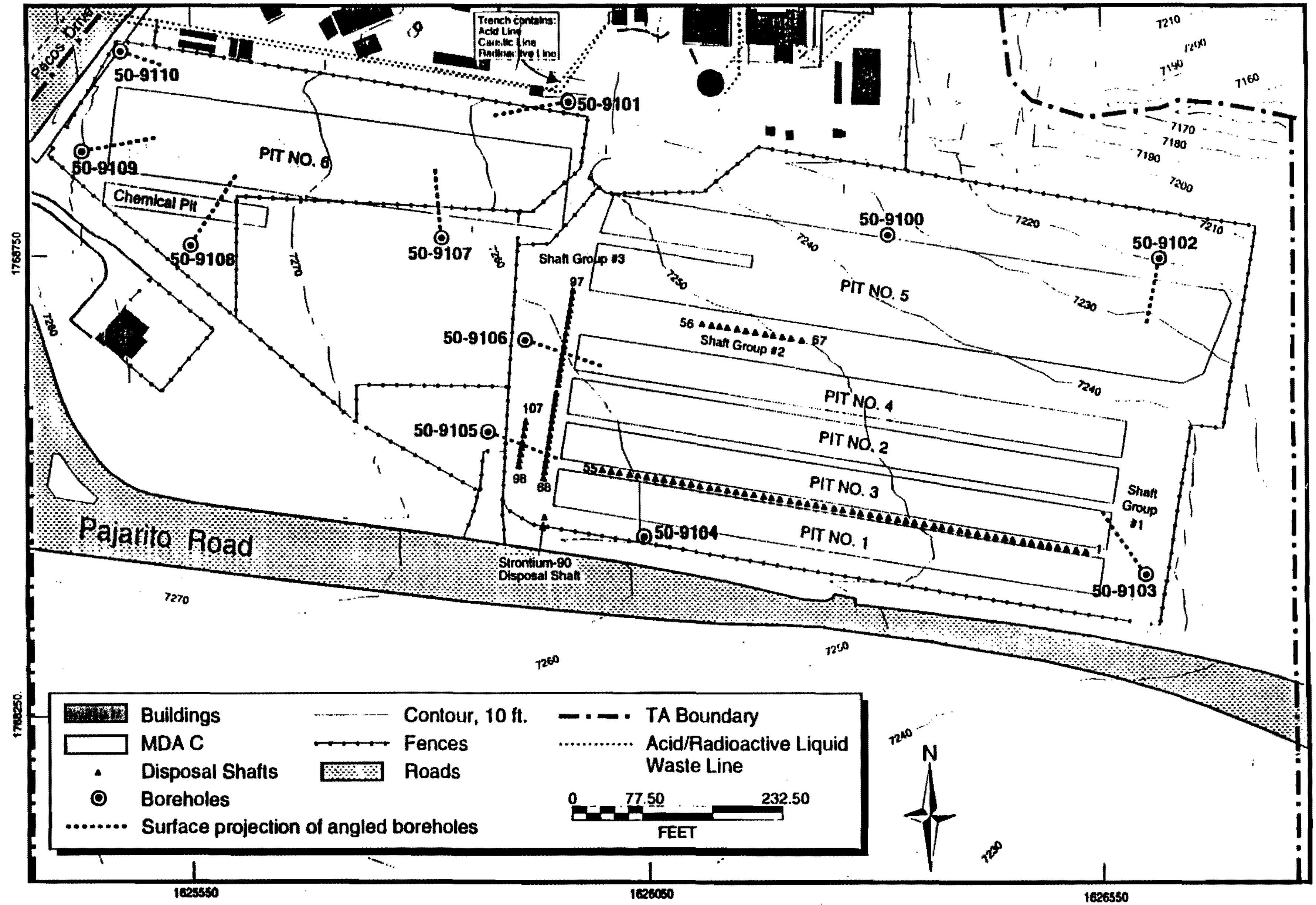

Figure A-3. Locations of RFI Boreholes Investigating Subsurface Disposal Units at MDA C.